SUPPLEMENTAL INFORMATION

Photic generation of 11-*cis*-retinal in bovine retinal pigment epithelium

Jianye Zhang[1, *], Elliot H. Choi[1,2, *], Aleksander Tworak[1, *], David Salom[1, *], Henri Leinonen[1], Christopher L. Sander[1,2], Thanh Hoang[3], James T. Handa[4], Seth Blackshaw[3,4], Grazyna Palczewska[5], Philip D. Kiser[6], Krzysztof Palczewski[1,#]

[1]Gavin Herbert Eye Institute, Department of Ophthalmology, University of California, Irvine, CA 92697;
[2] Department of Pharmacology, Case Western Reserve University, Cleveland, OH 44106;
[3] Solomon H. Snyder Department of Neuroscience, Johns Hopkins University School of Medicine, Baltimore, MD 21205;
[4] Department of Ophthalmology, Johns Hopkins University School of Medicine, Baltimore, MD 21287;
[5] Polgenix, Inc., Department of Medical Devices, 5171 California Ave., Suite 150, Irvine, CA 92617;
[6] Department of Physiology and Biophysics, University of California, Irvine, CA 92697, and the Research Service, VA Long Beach Healthcare System, Long Beach, CA 90822.

*equal contributions

Running title: Generation of 11-cis-retinal in retinal pigment epithelium

[#]To whom correspondence should be addressed: Krzysztof Palczewski, Ph.D.: Gavin Herbert Eye Institute, Department of Ophthalmology, University of California, Irvine, CA 92697; kpalczew@uci.edu; Tel: (949) 824-6527; Fax: 949-824-4015.

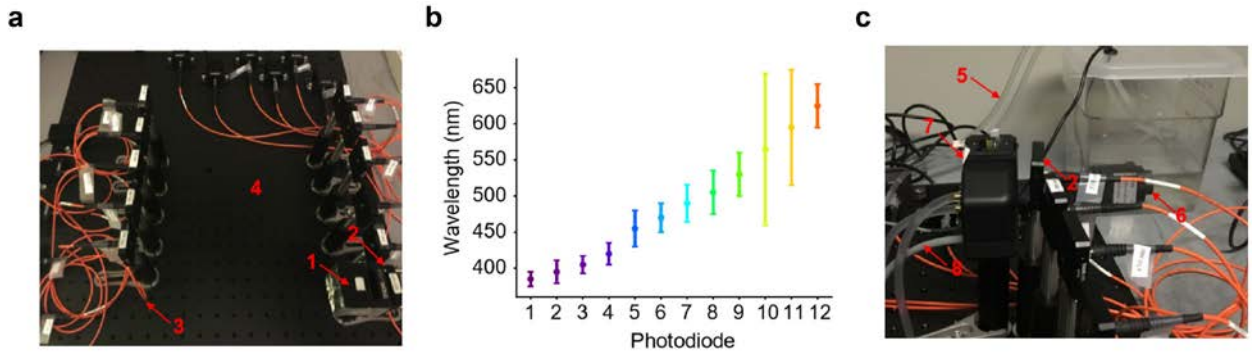

Supplementary Figure 1. Illumination system used in his work. (**a, b**) LEDs mounted on the optical breadboard (**a**) and their corresponding wavelengths (**b**); error bars indicate the range of wavelength emitted by each LED. 1, cuvette holder; 2, fiber fastened into CP02 cage plate with SM1SMA fiber adapter; 3, fiber to diode; 4, optical breadboard to rigidly hold equipment. (**c**) Temperature controlling system. 2, fiber fastened into CP02 cage plate with SM1SMA fiber adapter; 5, circulating pipe; 6, pump; 7, temperature-controlled cuvette holder; 8, cable to temperature controller.

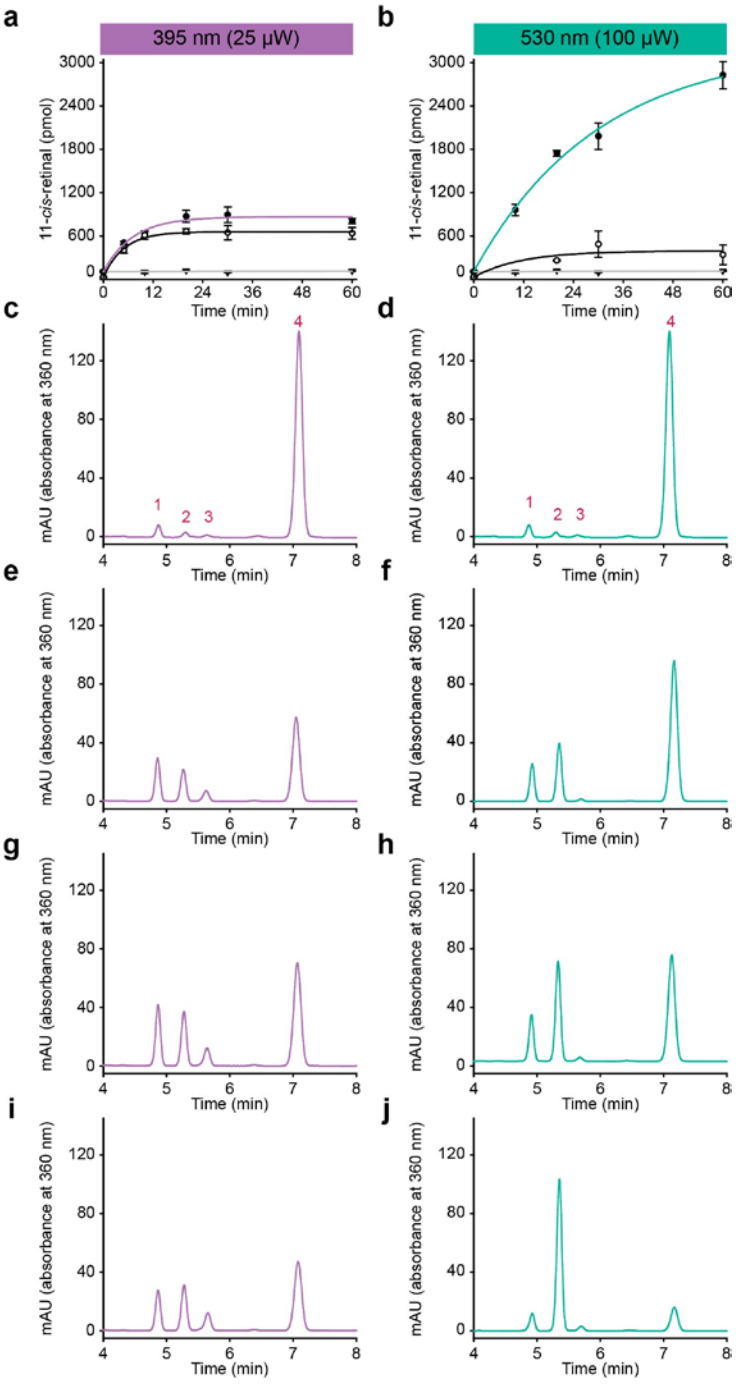

Supplementary Figure 2. **Photoisomerization of all-*trans*-retinal in the presence of RPE microsomes at 395 nm and 530 nm light.** (**a, b**) Time course of 11-*cis*-retinal generation under 25 µw of 395-nm light (**a**) and 100 µw of 530-nm light (**b**). 11-*cis*-retinal production was investigated with native retinal pigment epithelium (RPE) (●) or denatured RPE (○) under light, or native RPE under dark (∇). (**c-j**) Representative chromatographs of retinals extracted from samples exposed to 395 nm light for 0 (**c**), 10 (**e**), 20 (**g**) and 60 (**i**) min or 530 nm light for 0 (**d**), 10 (**f**), 20 (**h**), and 60 (**j**) min. Peak 1, 13-*cis*-retinal; peak 2, 11-*cis*-retinal; peak 3, 9-*cis*-retinal; peak 4, all-*trans*-retinal. Data points are shown as means ± standard deviations (n = 3).

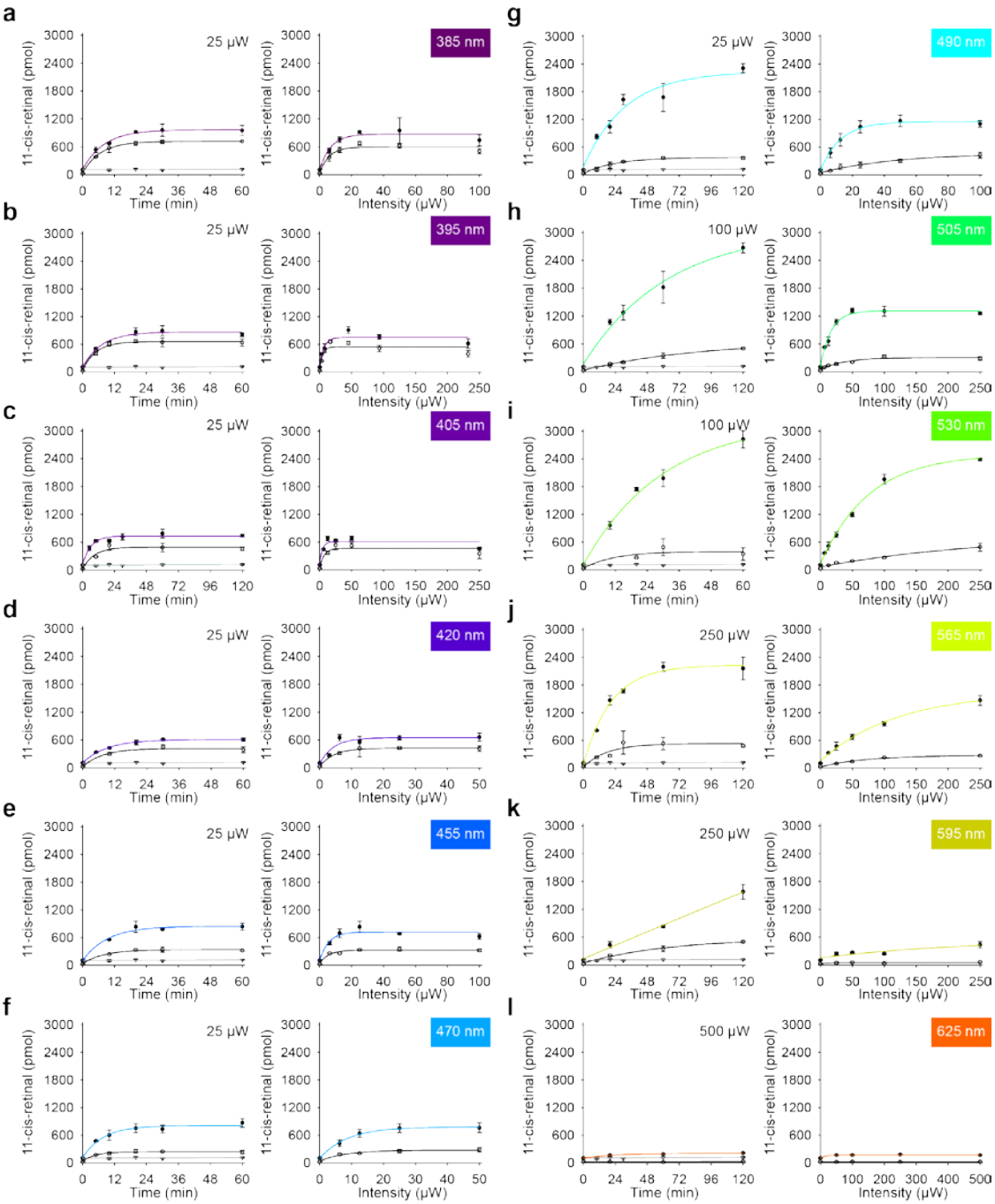

Supplementary Figure 3. **Profile of isomerization at different wavelengths.** The production of 11-*cis*-retinal in the presence of RPE microsomes was investigated under light with varying wavelength and fixed light intensity (indicated in panels) or set exposure time to 20 min (●, colored lines); the colors represent the wavelength of the light source. Generation of 11-*cis*-retinal with denatured RPE under the same conditions (○, black lines). The difference between the two values reflects the enzymatic 11-*cis*-retinal generation. 11-*cis*-retinal levels in the dark (∇ , gray lines) served as a negative control. Data points are shown as means ± standard deviations (n = 3).

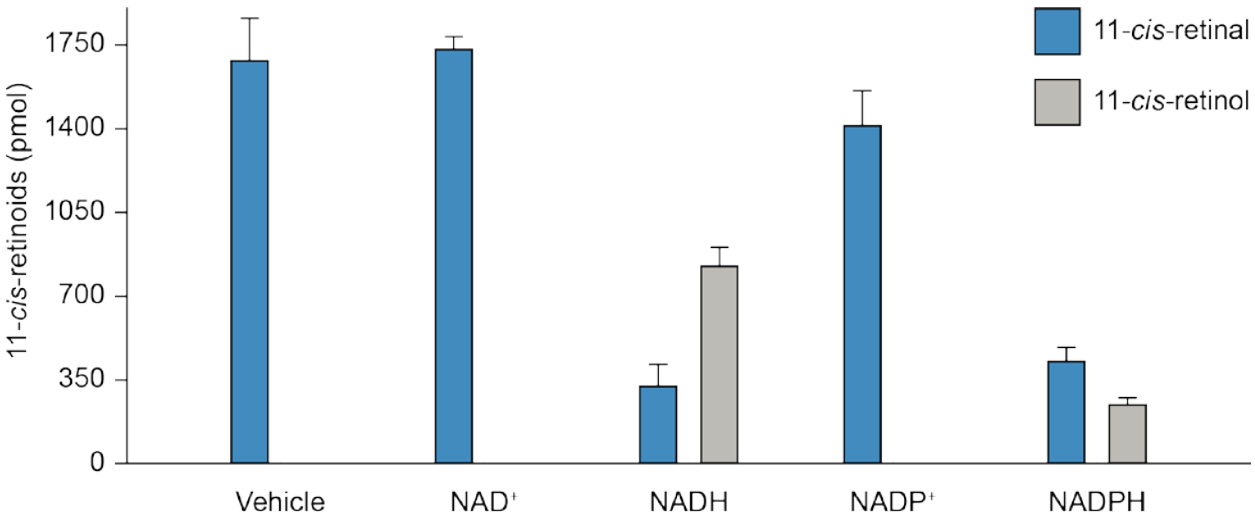

Supplementary Figure 4. **Photoisomerization in the presence of di-nucleotide cofactors.** Photoisomerization was carried out in the presence of NAD^+/NADH/$NADP^+$/NADPH (2 mM) with the light exposure set at 530 nm (100 µW) for 15 min. An excess of emixustat (10 µM) was added to inhibit the classic visual cycle. All the 11-*cis*-retinoids were quantified. The production of 11-*cis*-retinyl ester was negligible. The generation of 11-*cis*-retinol (**gray bars**) was only detectable in the presence of NADH/NADPH. The generation of 11-*cis*-retinal (**blue bars**) was mildly altered by the reducing cofactors. Data points are shown as means ± standard deviations (n = 3).

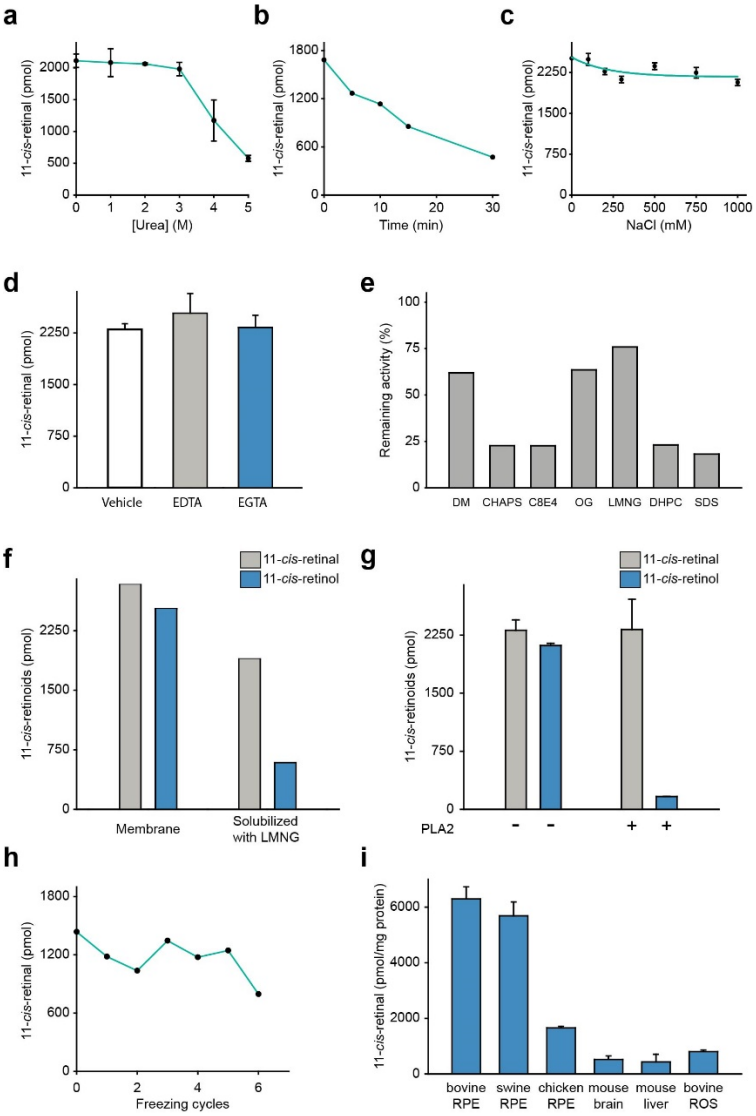

Supplementary Figure 5. **Properties of the photoisomerase.** Photoisomerization was carried out with the light exposure set at 530 nm (100 µW) for 15 min. (**a**) The activity of the photoisomerase after washing RPE membranes with urea. (**b**) The effect of trypsin digestion of RPE on the photoisomerase activity. (**c**) The solubilized photoisomerase activity is not affected by a high concentration of salt. (**d**) The impact of transition metal chelators on the photoisomerization activity of RPE. (**e)** Summary of detergent screening for RPE membrane solubilization. The solubilized photoisomerase activity was measured immediately after the RPE microsomes were solubilized with minimal amounts of detergent at 4 ºC, and again 12 h later. (**f**) Solubilization of RPE membranes inhibited RPE65 activity, in contrast to the photoisomerase activity. (**g**) Treatment with PLA_2 diminished 11-*cis*-retinol production (**blue bars**) by RPE65, while minimally altering 11-*cis*-retinal production (**gray bars**). (**h**) The influence of freeze-thawing cycles on the photoisomerization activity of solubilized RPE. (**i**) Photoisomerase activity varies between different tissues and species. (ROS: rod outer segments). Data points are shown as means ± standard deviations (n = 3).

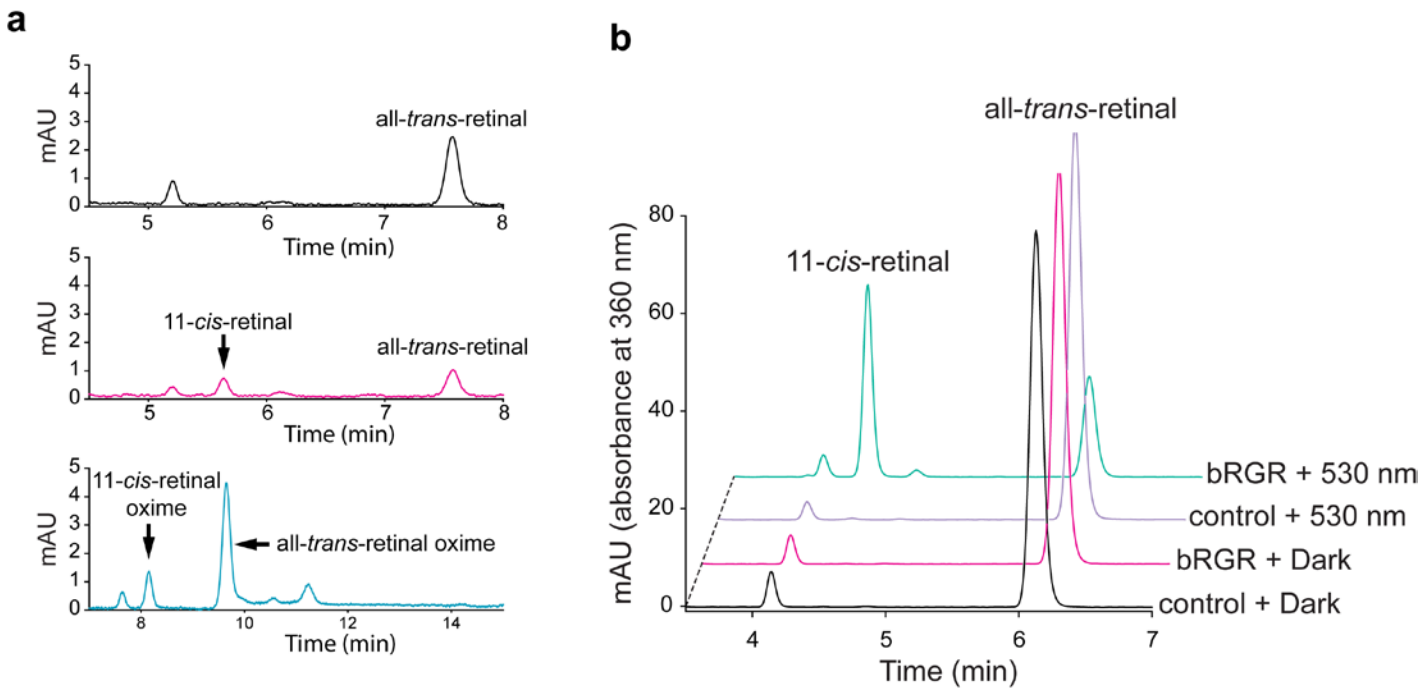

Supplementary Figure 6. HPLC analyses of isomerase activity of immunopurified bovine RGR expressed in HEK293S GnTI$^-$ cells. The data are related to **Fig. 8**. **(a)** HPLC analysis of retinoids corresponding to three of the spectra from **Fig. 8b;** each corresponding pair (spectrum-HPLC trace) has the same color coding. **(b)** Representative chromatograms corresponding to **Fig. 8c**, showing the change in retinoid content upon 530 nm light exposure.

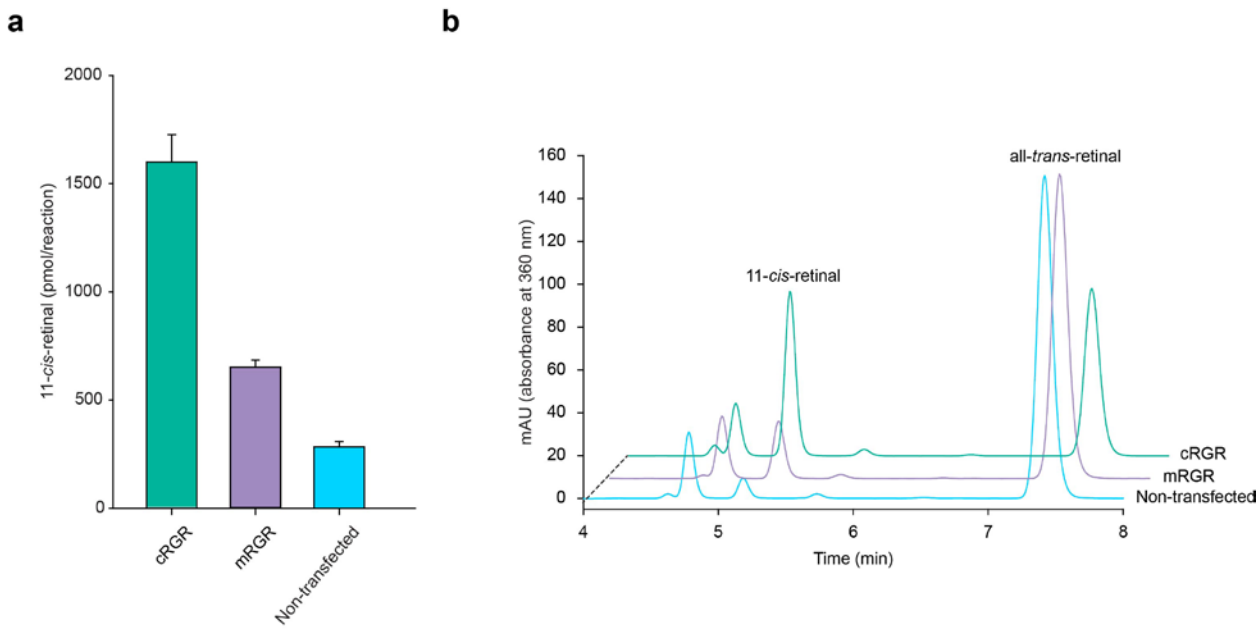

Supplementary Figure 7. Photoisomerase activity of chicken RGR and mouse RGR expressed in HEK293S GnTI$^-$ cells. (**a**) Amounts of 11-*cis*-retinal produced by photoisomerization from all-*trans*-retinal in cell homogenates exposed to 530 nm light in the presence of CRALBP. Homogenates of HEK293S GnTI$^-$ cells transfected with a plasmid encoding cRGR produced a significant amount of 11-*cis*-retinal. However, homogenates of cells transfected with a plasmid encoding mRGR produced relatively low amounts of 11-*cis*-retinal. n = 3 for the cRGR, n = 4 for the mRGR, n = 3 for the non-transfected. Data are shown as mean ± standard error of the mean. (**b**) Representative chromatograms showing the change in retinoid content upon 530 nm light exposure.

Supplementary Table 1. List of bovine proteins identified in the MS analysis of an approximately 27 kDa band visible after SDS-PAGE analysis of proteins purified from RPE microsomes (Fig. 5d).

Accession (UniProt)	Protein name	MW (kDa)	Coverage	Uniqe Peptides	# of PSMs
P47803	RPE-retinal G protein-coupled receptor	31.9	52.92%	11	130
Q3T149	Heat shock protein beta-1	22.4	60.20%	10	22
Q3ZBK2	Redox-regulatory protein FAM213A	24.3	38.53%	8	19
P06394	Keratin, type I cytoskeletal 10	54.8	11.79%	7	15
Q17QC0	Membrane-associated progesterone receptor component 1	21.6	40.21%	9	14
Q29455-2	Isoform CSP2 of DnaJ homolog subfamily C member 5	18.8	19.16%	4	12
Q5XQN5	Keratin, type II cytoskeletal 5	62.9	10.15%	4	11
Q0IIG7	Ras-related protein Rab-5A	23.7	33.49%	3	11
A5PKI3	Protein FAM3C	24.8	26.43%	6	10
Q58DS9	Ras-related protein Rab-5C	23.5	26.85%	2	9
Q3MHP2	Ras-related protein Rab-11B	24.5	29.82%	6	8
A7MBI7-2	Isoform 2 of Catechol O-methyltransferase	24.8	19.00%	3	7
A1L595	Keratin, type I cytoskeletal 17	48.7	8.16%	2	7
Q17R06	Ras-related protein Rab-21	24.1	16.67%	3	7
P60712	Actin, cytoplasmic 1	41.7	12.53%	4	6
Q29S21	Keratin, type II cytoskeletal 7	51.5	8.37%	2	6
Q32LM6	Protein lin-7 homolog A	26	17.60%	4	5
Q1JQ93	Dolichol-phosphate mannosyltransferase subunit 1	29.6	18.46%	4	5
Q8MJG0	Regulator of G-protein signaling 9-binding protein	25.7	14.77%	3	5
Q27979	11-cis retinol dehydrogenase	35	11.64%	3	5
Q08D83-2	Isoform 2 of Reticulon-3	25.5	8.02%	2	5
A1A4R1	Histone H2A type 2-C	14	20.16%	2	4
Q3ZBR9	Ermin	32.4	9.93%	2	4
P11023	Ras-related protein Rab-3A	24.9	19.09%	3	4
P62808	Histone H2B type 1	13.9	19.05%	2	3
Q95JH2	1-acyl-sn-glycerol-3-phosphate acyltransferase alpha	32	6.62%	2	3
A7E3W5	Synaptogyrin-2	25.1	8.48%	2	3
Q3T004	Serum amyloid P-component	25.2	9.82%	2	2
Q3T189	Succinate dehydrogenase [ubiquinone] iron-sulfur subunit, mitochondrial	31.5	7.14%	2	2
Q2TBW7	Sorting nexin-2	58.4	5.20%	2	2

Supplementary Table 2. List of PCR primers used in the study.

Site-directed mutagenesis	
Name	Sequence (5'-3')
BOVRGR_K255A_FW	TCTCATTGCCGCCGCAGTACCCACAGTCAACGC
BOVRGR_K255A_RV	GCGGGCACCATCTGCAGC
HUMRGR_K255A_FW	CCTCATTGCCGCCATGGTGCCCACGATC
HUMRGR_K255A_RV	GCGGGCACCATCTGCAGT